MicroBooNE: Neutron Induced Cosmogenic π^0's

Ryan A.Grosso

Submitted in partial fulfillment of the
requirements for the degree
of Doctor of Philosophy
in the Graduate School of Arts and Sciences

UNIVERSITY OF CINCINNATI

2017

Table of Contents

List of Figures **iii**

List of Tables **iv**

1 Introduction **1**

2 Neutrinos & Neutrino Oscillations **2**

3 The MicroBooNE Detector **3**

4 Booster Neutrino Beam **4**

5 Low Energy Excess and Relevant Cross Sections **5**

6 Cosmogenic π^0's at MicroBooNE **6**

6.1 Motivation 6

6.2 Traditional Reconstruction 8

6.3 Wire Cell Imaging 9

6.4 Pattern Reconcition 10

6.4.1 Clustering 11

6.5 Track and Shower Selection 13

6.5.1 Track Removal 13

6.5.2 Single π^0Reconstruction 13

6.6 Single π^0cosmic sample 16

7 Results **20**

8 Conclusions **21**

8.1 Conclusion 21

8.2 Outlook 21

I Appendices **22**

List of Figures

6.1 Icarus Cosmic π^0 8
6.2 Wire Cell reconstruction of CORSIKA MC viewed in the BEE viewer . . . 11
6.3 The image on the left shows a muon track in 12
6.4 Shower merging graphic 13
6.5 pi0Photon 14
6.6 Reconstructed energy sum and energy product for shower pairs 15
6.7 pi0Photon 16
6.8 pi0Photon 17
6.9 Cosmic π^0production by parent process 18
6.10 pi0Photon 19

List of Tables

Chapter 1

Introduction

Chapter 2

Neutrinos & Neutrino Oscillations

Chapter 3

The MicroBooNE Detector

Chapter 4

Booster Neutrino Beam

Chapter 5

Low Energy Excess and Relevant Cross Sections

Chapter 6

Cosmogenic π^0's at MicroBooNE

In this chapter we will talk about some of the challenges and interesting physics cases regarding cosmogenics in a surface LArTPC. Many cosmic ray particles penetrate surface detectors and populate the detector region making it necessary to remove these particles from reconstruction and address charge contamination in neutrino events. The majority of this chapter will emphasize cosmogenic track removal, electromagnetic showers and subsequently π^0selection. We will first examine some historical cosmogenic studies from the Icarus experiment.Then, introduce what MircoBooNE can contribute in terms of understanding cosmics. We will address the cosmic simulation that is used, various steps in reconstruction and pattern recognition used to select π^0's in a LArTPC. Finally, we will conclude with how these studies impact future cross section analyses and backgrounds toward the low energy excess analysis.

6.1 Motivation

Cosmogenic particles allow for a separate test of reconstruction tools along with an independent way to address detector energy scale. The high rate of surface cosmics do indeed cause some trouble with disentangling signal neutrino events so cosmic ray removal Luckily, surface cosmogenic samples allow for a large statistics dataset to develop and optimize reconstruction techniques. Cosmogenic muons that traverse the detector provide a handle to understand detector energy scale along with understanding track reconstruction efficiency.

Stopping muons that produce a Michele electron help provide a benchmark for low energy showers in the 10's of MeV range. The π^0resonance, with a mass of $134.9 MeV/c^2$, can be used as a standard candle to benchmark overall detector energy scale.

$$\mathcal{M} = \sqrt{2E_1E_2(1-\cos\theta_{12})} \tag{6.1}$$

Electromagnetic shower reconstruction for LArTPC's is well known to be a hard task. The high resolution of the 2-dimensional projections of EM-showers introduce many challenges to develop unbiased and fully automated reconstruction. In 2001, the T600 ICARUS detector **??** performed a surface test run in Pavia, Italy. During this 100 day test the detector collected over 30,000 cosmic ray events. In 2008, the ICARUS collaboration published a study of electromagnetic showers coming from π^0decays in the Pavia dataset. To select candidate π^0events, ICARUS hand scanned a total of 7,500 potential events from a PMT triggered sample. Their hand scanning requirements included, that at least two well separated electromagnetic showers were visible, a valid t_0 time for the vertex, and that there was not much charge contamination coming from a nearby cosmic muon. After this, they were left with 212 'hadronic interactions with at least one candidate neutral meson' which they then proceeded to reconstruct. Their final reconstruction consisted of energy scaling to account for missing charge in the shower and a minimization against the true π^0mass (134.9). An example of one of their hand scanned clustering events is shown if Figure 6.1.

MicroBooNE, being a surface detector, is in a position to do a similar study with improved reconstruction techniques. Also, understanding the cosmic production rate for single π^0's is valuable to any MicroBooNE analysis that involves EM-showers. The following sections will present MicroBooNE's Monte Carlo simulation and state of the art reconstruction techniques.

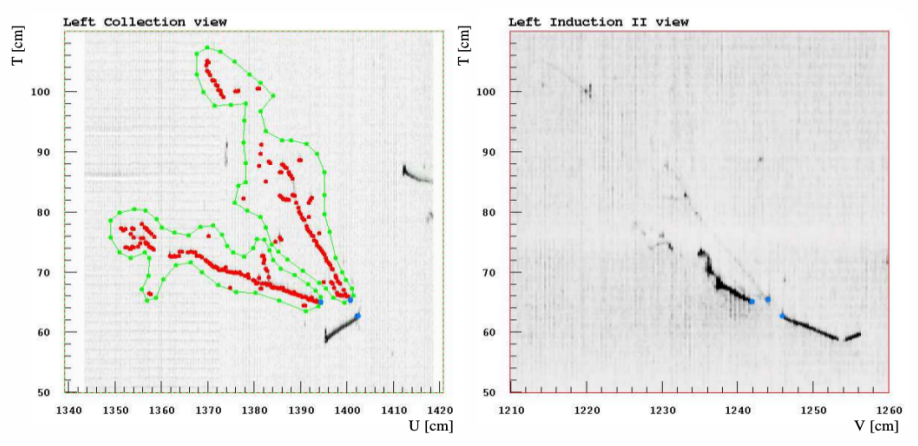

Figure 6.1: A cosmic $\pi^0$from the ICARUS Pavia run. The left image, shows the hand drawn clustering and positions of the shower conversion point and vertex point. The right image, shows the same event on a different wire plane view.

6.2 Traditional Reconstruction

The traditional approach for LArTPC reconstruction involves grouping drift charge that is deposited on the wires to form wire-hits. The light collection system also has light-hits which corresponded to collected light on an individual. A group of PMT's that have light-hits at the same time is called a flash. Hits from each of the wire planes are clustered together with various reconstruction algorithms to form reconstruction objects that relate to individual particles in the detector. There are two primary reconstruction objects: tracks, which are mostly linear and compact clusters that represent muons, protons, and charged pions, and showers which are more fuzzy shaped cluster objects that represent photons and electrons. Next, to reconstruction a 3D object, an algorithm must match the same 2D cluster objects in at least two of the three wire planes. For MicroBooNE, and the general LArTPC community, matching track reconstruction well advance but shower reconstruction suffers many hurdles. In recent years lots of progress has been made for LArTPC shower reconstruction. Various different techniques such as: improved 2D clustering and matching techniques[], sophisticated pattern recognition tools[] , and deep learning[] approaches have been explored with various strengths and weaknesses.

6.3 Wire Cell Imaging

The traditional approach is not the only way to reconstruct LArTPC data. Instead, wire data can be treated with a tomographic approach directly producing a set of 3D space points. Although computationally intensive, this approach allows for more information to be used in a 3D clustering framework which can directly impact shower reconstruction and mitigate degeneracies from the 2D matching method.

The Wire-Cell framework, spearheaded by Brookhaven National Labs(BNL), utilizes this approach to create 3D space points from MicroBooNE's TPC data. The approach relies on the assumption that the same amount of ionization charge is seen on each plane. In MicroBooNE this is done by reconstructing small time slices on each wire planes. Each time slice involves solving a charge equation for all possible hits with respect to the matrix of hits actually recorded in the time slice. The charge equation is shown in equation 6.2. The detector wire signals are represented in matrix W while all potential wire hits are contained in H. Nonzero values in the Q matrix will correspond to unique wire-plane intersections of charge, near zero values represent ghost hits due to degeneracies in the charge equation.

$$\begin{bmatrix} W_{u_1} \\ \vdots \\ W_{u_n} \\ W_{v_1} \\ \vdots \\ W_{v_n} \\ W_{y_1} \\ \vdots \\ W_{y_n} \end{bmatrix} = \begin{bmatrix} Q_{u_1}^{H_1} & Q_{u_1}^{H_2} & \cdots & \cdots & \cdots & Q_{u_1}^{H_{m-1}} & Q_{u_1}^{H_m} \\ \vdots & \vdots & \ddots & \ddots & \ddots & \vdots & \vdots \\ Q_{u_n}^{H_1} & Q_{u_n}^{H_2} & \cdots & \cdots & \cdots & Q_{u_n}^{H_{m-1}} & Q_{u_n}^{H_m} \\ Q_{v_1}^{H_1} & Q_{v_1}^{H_2} & \cdots & \cdots & \cdots & Q_{v_1}^{H_{m-1}} & Q_{v_1}^{H_m} \\ \vdots & \vdots & \ddots & \ddots & \ddots & \vdots & \vdots \\ Q_{v_n}^{H_1} & Q_{v_n}^{H_2} & \cdots & \cdots & \cdots & Q_{v_n}^{H_{m-1}} & Q_{v_n}^{H_m} \\ Q_{y_1}^{H_1} & Q_{y_1}^{H_2} & \cdots & \cdots & \cdots & Q_{y_1}^{H_{m-1}} & Q_{y_1}^{H_m} \\ \vdots & \vdots & \ddots & \ddots & \ddots & \vdots & \vdots \\ Q_{y_n}^{H_1} & Q_{y_n}^{H_2} & \cdots & \cdots & \cdots & Q_{y_n}^{H_{m-1}} & Q_{y_n}^{H_m} \end{bmatrix} \begin{bmatrix} H_1 \\ H_2 \\ \vdots \\ \vdots \\ \vdots \\ \vdots \\ \vdots \\ H_{m-1} \\ H_m \end{bmatrix} \tag{6.2}$$

Then, each 'slice' is stacked to it's corresponding x position. This produces a set of 3D space points that can used in patter recognition algorithms to identify different particles in the data. All reconstruction is done with accounting for known detector dead regions, the current state of MicroBooNE's signal and noise processing and imaging that requires a minimum of 2 to be matched from the charge equation.

6.4 Pattern Reconcition

Various pattern recognition tools are needed to address MircoBooNE's TPC data but for this analysis they can be generalized into two efforts, cosmic track removal and EM-shower clustering. Both approaches require different techniques. First, we will focus on optimizing track removal. This involves identifying tracks that are thoroughgoing, and contained. Once all the charge associated with tracks are removed, the remaining charge is clustering into candidate EM-shower objects. Finally, correlated shower pairs are identified and selected as candidate π^0events.

A image of a typical MicroBooNE cosmic event reconstructed with 3D wire cell space points are shown in Figure 6.2 using the BEE viewer []. A detailed list of reconstruction and selection parameters are listed in appendix **??**

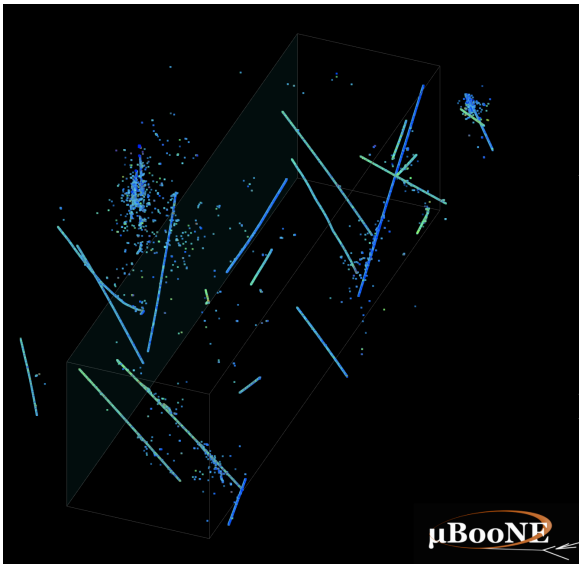

Figure 6.2: This is a typical cosmic event in the MicroBooNE detector. The data used to generate this event is CORSIKA MC.

6.4.1 Clustering

The wire cell data produces a set of 3D space points as mentioned in section 6.3. Only space points that are in the fiducial volume are clustered and considered in the reconstruction process. First a threshold cut of 500 Q is applied to all the remaining space points. This is does to remove very low charge ghost points and reduce the overall number of points to cluster. The main goal of this step is to identify the large scale structure of the cosmic tracks in the data. Additionally, with a smaller number of space points the computational time for reconstruction is reduced.

The first stage of clustering uses BIRCH (balanced iterative reducing and clustering using hierarchies). The hyper parameters were tuned such that cosmic tracks are removed with minimal impact to showers involved from π^0. Birch clustering was chose because it scales well with large number of points, efficiently maintains large number of clusters in datasets and also handles outliers removal well. This clustering technique leverages on the inherent structure of track like particles. Particles such as protons, muons, and charged pions are are continuously ionizing meaning that there should be not be gaps of charge. This feature is much different than EM-showers which have lots of gaps between where

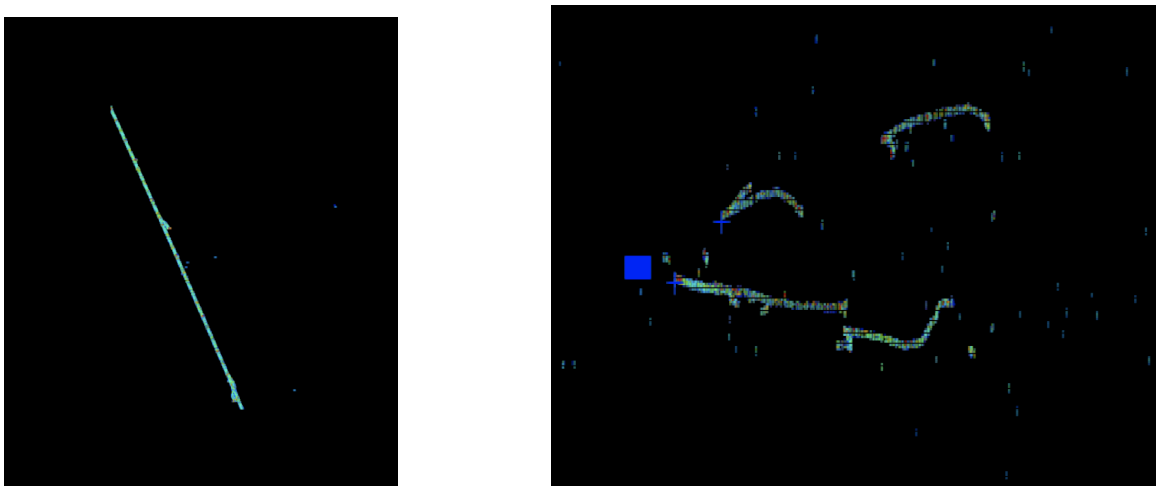

(a) Title A (b) Title B

Figure 6.3: The image on the left shows a muon track in

charge is deposited. An example of this is shown in figure 6.3

The next stage of the clustering process is to merge together clusters that did not get fully clustered in the BIRCH clustering step. The second pass clustering is geared toward larger object clustering. To address this, a 3D convex hull is constructed around every cluster. Next, the euclidean distance of the vertex points are calculated, if a pair of points from two separate clusters are within a minimum distance then the clusters are merged together. If the minimum merging distance is small, the clusters from tracks get merged together well while clusters from showers still need further merging.

The final stage of clustering is shower clustering. This requires there to be a distinction between a cluster object that is shower-like or track-like. To do this, cluster parameters are made produced for every cluster. The most important features from the cluster parameters are cluster length and spread of the first principle component. More details about track and shower selection are described later in section 6.5. Shower clustering involved

Once defined as a shower cluster, a 3D charge weighted axis is fit to the cluster's set of space points. First, a distance of closest approach(DOCA) for each cluster axis pair is calculated and a protovertex is calculated at the midpoint of the DOCA line. Next, a unique conversion point is calculate for each shower pair to serve as a proxy for radiation length. Using the protvertex point and two conversion points an opening angle is calculated. A pair

of clusters that have a DOCA that is less than 5CM, an angle between 15 and 165 degrees, and both of the radiation lengths are less than 20cm are merged together. The merging is done for all shower cluster pairs and

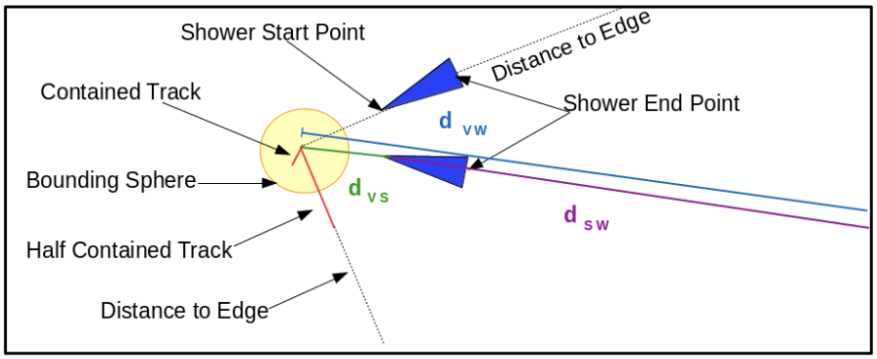

Figure 6.4: This graphic illustrates all the data objects and relevant parameters. The shower objects are shown in blue, track objects shown in red, and a bounding sphere, used to associate tracks with the vertex, is shown in yellow.

6.5 Track and Shower Selection

6.5.1 Track Removal

For this analysis track removal is handled in a unique manor. The primary goal is to identify showers coming from a π^0. Therefore, all cuts and optimizations will be tested against shower objects. The general approach for track removal depends heavily on geometric properties such as length and linearity of the cluster.

6.5.2 Single π^0Reconstruction

The vast majority(98.8%) of π^0's decay into two photons. The relationship for the particle mass, which was defined in eq6.1, shows the importance of properly account for the energy and angle between the decay photons. To understand a baseline for reconstruction efficiency we have generated a sample of 10000 single particle events isotropically throughout the detector volume with initial momentums spanning from 0 to 2 GeV.

First we will investigate energy deposited in detector from the decay. An plot of the true kinematic energy of photons from the decay particle is shown in Figure 6.5. It is important to note that both photons need to be reconstructed to form a mass resonance. This means that we are driven to optimize reconstruction to be robust around showers in the range of many 10's of MeV in deposited energy. Photons that convert near the fiducial edge of the detector can escape and deposit a small amount of energy in the detector. This poses problems for capturing the total amount of energy of the shower and drives the need for a fiducial cut around the edges.

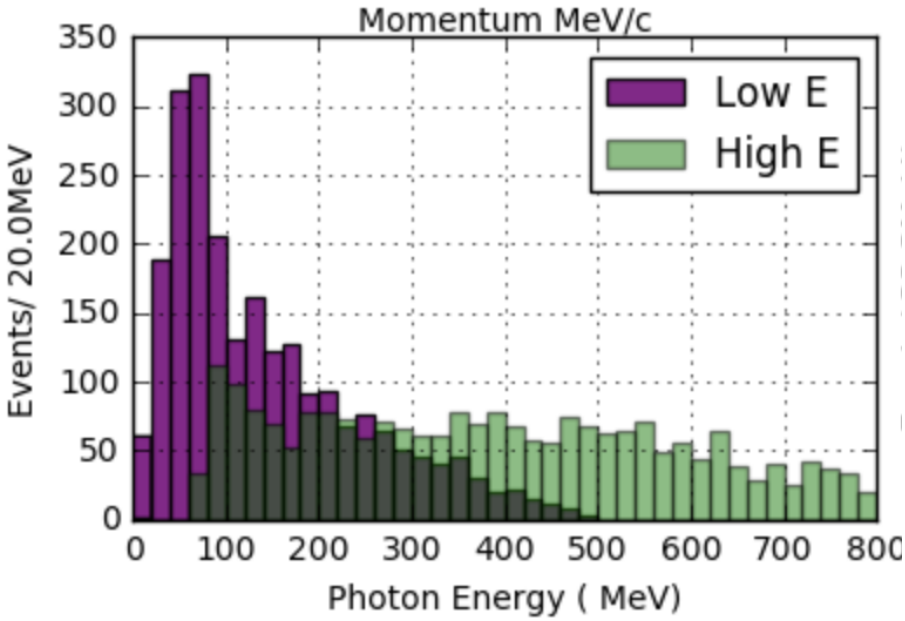

Figure 6.5: The

To plot reconstruction accuracy for the energy we are most interested in two metrics. The first, is the sum of energy collected between the two showers. This informs us that we are accounting for most of the energy deposited and handling the fiducial cuts well. The second, is the product of the two shower energies. This directly impacts the reconstructed mass resolution and informs us that we are properly clustering energy between the two showers properly. In figure 6.6 both metrics are plotted for reconstruction against true. Points along the diagonal represent accurate model predictions. As we will see later in this

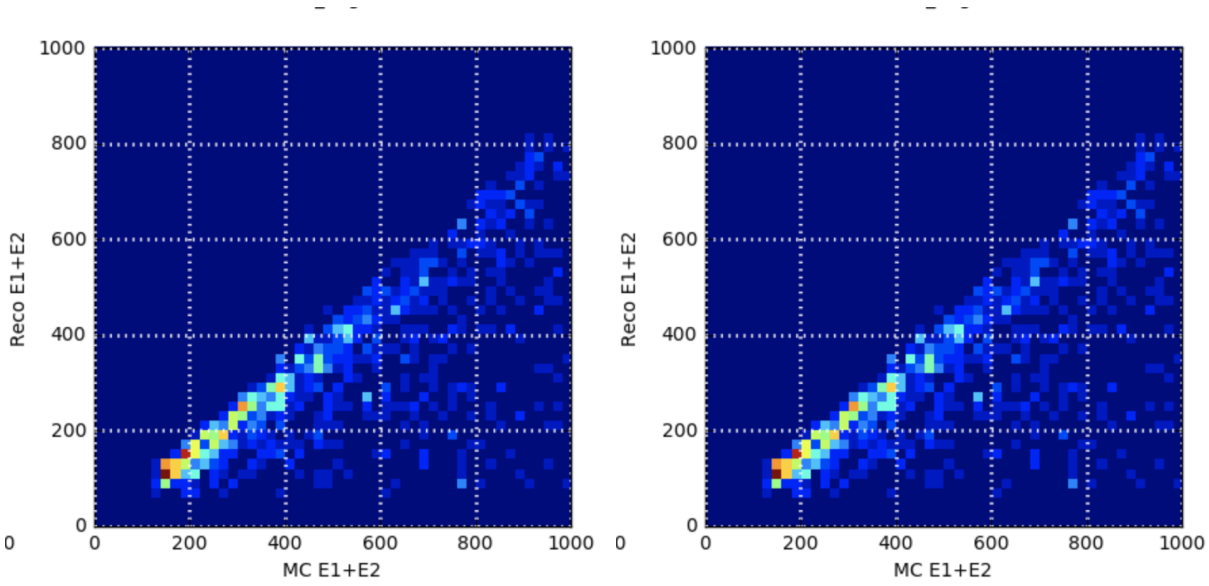

(a) Title A

(b) Title B

Figure 6.6: Reconstructed energy sum and energy product for shower pairs

chapter, the energy product drives the width of the mass resolution.

Next we will investigate the effects of the opening angle between the two photons. The minimum opening angle of the photons is constrained by the momentum boost as the particle decays as shown in equation 6.3. The angular resolution is a very challenging problem in LArTPC's using the traditional 2D projection approach. Fortunately, direct 3D reconstruction improves the angular resolution and allows for a better measurement of shower direction.

$$\sin\frac{1}{2}\theta_{min} = \frac{M}{E_{\pi^0}} \tag{6.3}$$

A plot of the reconstructed vs true opening angle is shown in Figure 6.10. The $1 - cos\theta$ term from equation 6.1 is sensitive to tails of the mass distribution.

Finally we apply a final set of selection cuts. First, we require that the distance of closest approach between the two shower axis is less than 5 cm. This is to help ensure that the photons are originating from a common origin. Next, the photon conversion distance

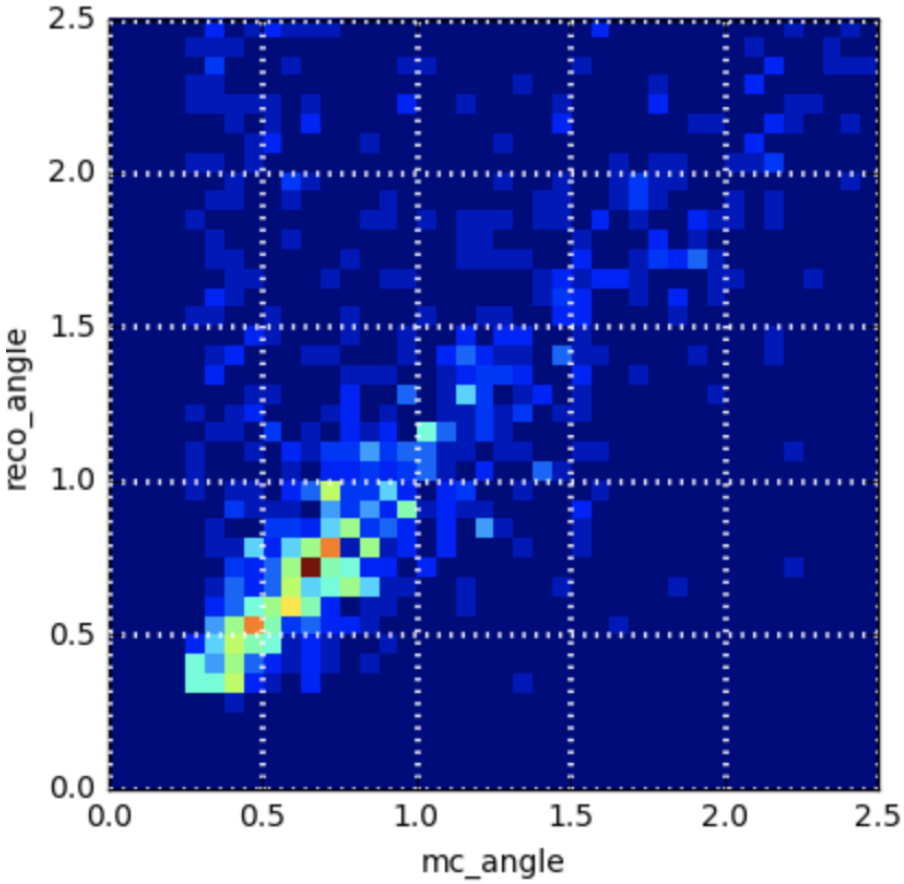

Figure 6.7: The

can not be longer than 70cm. This is done to help identify showers that are correlated from the same decay. Finally we only accept showers that are above 50 MeV in reconstructed energy. Figure 6.8 shows the effect of various parameters as applied to the reconstruction. We find that the deficit in mass peak is mainly due to the energy reconstruction. This is due to clustering effect from missing energy.

6.6 Single π^0cosmic sample

he MicroBooNE cosmics Monte Carlo is generated by CORSIKA(COsmic Ray Simulation for KAscade) v-7.4003[?] CORSIKA simulates particles coming from a wide range of interactions initiated by cosmic ray particles in the upper atmosphere. The simulation is

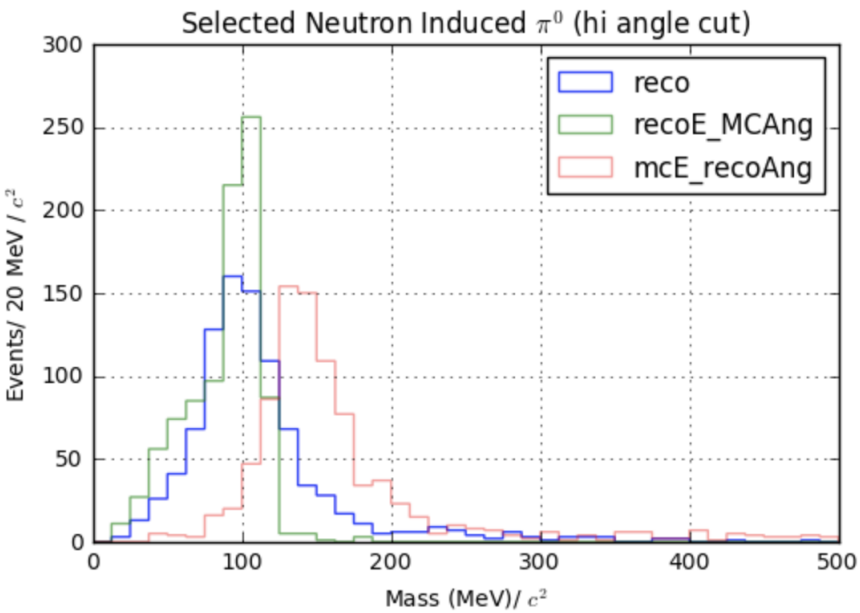

Figure 6.8: The reconstructed mass distribution is

robust and accounts for various input parameters such as, longitude and latitude, elevation, and the earths magnetic field. The particles are simulated over a large region above the detector complex but only particles that travel through the detector cryostat volume are kept. The passage of these particles simulated by the GEANT4 package. Cosmic rays that do not travel through the cryostat have a low likelihood of producing secondary or tertiary particles that enter the detector TPC volume[**?**]

In one MicroBooNE drift window(2.3ms) there are on average 6 cosmic muons. The muons do not directly contribute to many EM-showers but sometimes pass through an EM-shower from another particle. For MicroBooNE, the vast majority of muons are through-going and do not lead directly toward any method of π^0production.

Various other particles such as, protons, neutrons, and charged pions enter the TPC volume and may produce subsequent π^0. A distribution of π^0production process is shown in Figure6.9. Nearly half of the π^0's produced in the MicroBooNE TPC are produced through a neutron inelastic scattering.

talk about pi0 production dist in the detector.

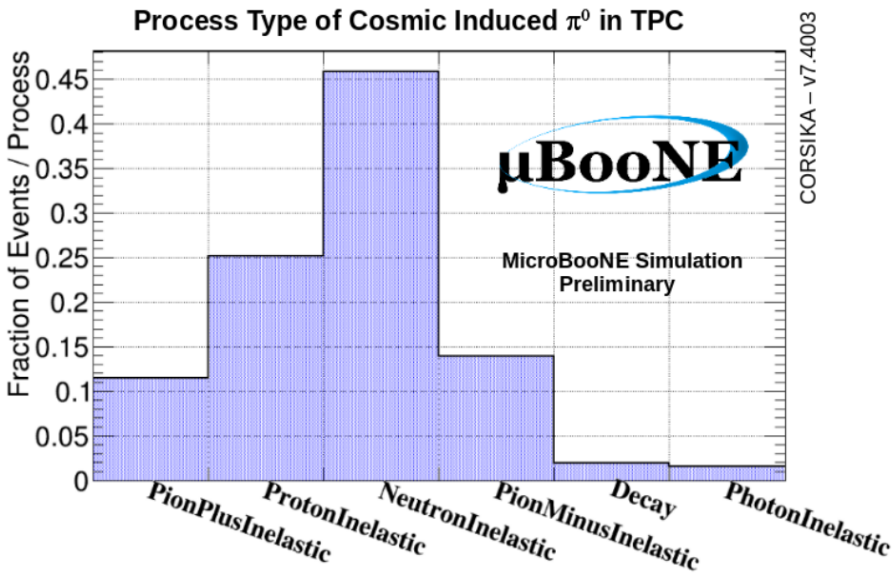

Figure 6.9: Physical process for cosmic π^0that decay inside the TPC.

248 Talk about background rates from MC.

249 show distributions from pi0 events w.r.t. signal.

250 Finally produce signal/background rates

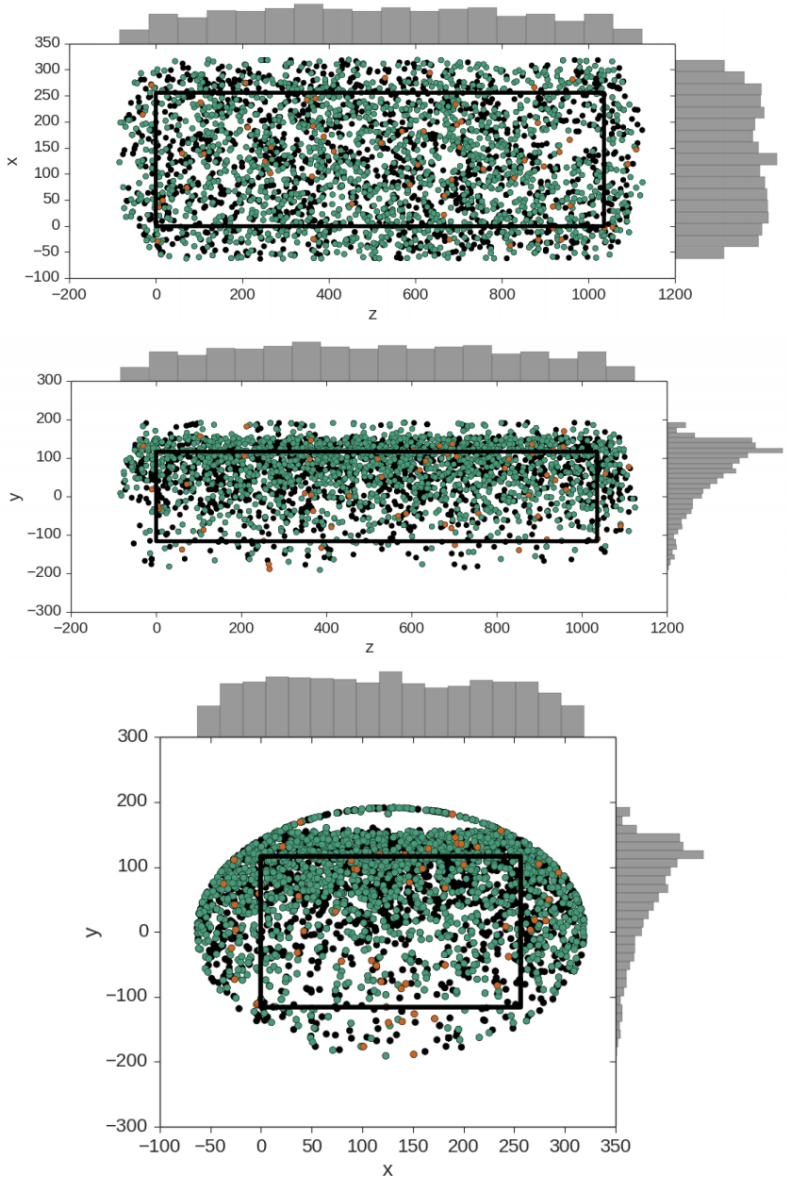

Figure 6.10: These plots show the decay point of actual cosmic π^0's throughout any time in the 4.8 ms window. The green points represent neutron induced π^0's, the orange represent photon induced π^0's, and the black represent a π^0that was produced from a charged particle. In each plot the black box is to represent the entire TPC dimensions not including fiducial cuts.

Chapter 7

Results

Chapter 8

Conclusions

8.1 Conclusion

We see that using a 3D approach is powerful in terms of reconstruction. more importantly we see the capilites of shower reconstruction with an LARTPC, and we see the extension of how this work leads to an NCpi0 cross section someday.

8.2 Outlook

Part I

Appendices